RESEARCH ARTICLE | *Obesity, Diabetes and Energy Homeostasis*

Enhanced oxidative capacity of ground squirrel brain mitochondria during hibernation

Mallory A. Ballinger,[1] Christine Schwartz,[1,2] and Matthew T. Andrews[1]

[1]*Department of Biology, University of Minnesota Duluth, Duluth, Minnesota; and* [2]*Department of Biology, University of Wisconsin-La Crosse, La Crosse, Wisconsin*

Ballinger MA, Schwartz C, Andrews MT. Enhanced oxidative capacity of ground squirrel brain mitochondria during hibernation. *Am J Physiol Regul Integr Comp Physiol* 312: R301–R310, 2017. First published January 11, 2017; doi:10.1152/ajpregu.00314.2016.—During hibernation, thirteen-lined ground squirrels (*Ictidomys tridecemlineatus*) regularly cycle between bouts of torpor and interbout arousal (IBA). Most of the brain is electrically quiescent during torpor but regains activity quickly upon arousal to IBA, resulting in extreme oscillations in energy demand during hibernation. We predicted increased functional capacity of brain mitochondria during hibernation compared with spring to accommodate the variable energy demands of hibernation. To address this hypothesis, we examined mitochondrial bioenergetics in the ground squirrel brain across three time points: spring (SP), torpor (TOR), and IBA. Respiration rates of isolated brain mitochondria through complex I of the electron transport chain were more than twofold higher in TOR and IBA than in SP ($P < 0.05$). We also found a 10% increase in membrane potential between hibernation and spring ($P < 0.05$), and that proton leak was lower in TOR and IBA than in SP. Finally, there was a 30% increase in calcium loading in SP brain mitochondria compared with TOR and IBA ($P < 0.01$). To analyze brain mitochondrial abundance between spring and hibernation, we measured the ratio of copy number in a mitochondrial gene (*ND1*) vs. a nuclear gene (*B2M*) in frozen cerebral cortex samples. No significant differences were observed in DNA copies between SP and IBA. These data show that brain mitochondrial bioenergetics are not static across the year and suggest that brain mitochondria function more effectively during the hibernation season, allowing for rapid production of energy to meet demand when extreme physiological changes are occurring.

mitochondria; brain; hibernation; proton leak; calcium uptake; thirteen-lined ground squirrel

HIBERNATION is an energy-conserving strategy employed by some mammals to withstand unfavorable environmental conditions (69, 93). For example, during hibernation, thirteen-lined ground squirrels (*Ictidomys tridecemlineatus*) enter a state of torpor in which their heart rate drops below 5% of their normothermic rate, they maintain a core body temperature as low as 5°C, and their cerebral blood flow is reduced by 90% (2, 38, 96). However, this state of reduced metabolism is periodically interrupted throughout the season by interbout arousals (IBAs), during which the ground squirrels briefly return to a physiological state typical of homeothermic mammals and nonhibernating periods for this species (22).

The processes of hibernation are regulated by various regions of the brain (reviewed in Ref. 31), and some regions stay active year round in thirteen-lined ground squirrels (12). For example, although overall glucose uptake by torpid ground squirrel brain is reduced to 1–2% of active control values (38), the relative utilization of glucose by the suprachiasmatic nucleus (SCN), an important regulator of the hibernation circuitry, remains higher than that of most other brain regions during deep torpor (55). This necessitates at least a low-baseline energy demand during torpor. Additionally, ground squirrel hypothalamus and brain cortex undergo changes in glucose uptake during transitions between torpor and IBA (54). Similarly, c-Fos expression, which is used as a marker of neuronal activation, was elevated during torpor in the SCN, again suggesting at least some energy demand during torpor (12). However, reducing or eliminating function in nonvital brain areas serves to conserve energy (27). Cortical electroencephalogram recordings during torpor indicate that there is little to no activity occurring during this time (108). A previous finding that synaptic connections are significantly reduced in some areas of the forebrain during torpor also supports this observation (106). Similarly, changes in dendritic spines and other synaptic structures resulting in reduced connectivity have been shown in torpor as well (70, 85, 86, 105). To illustrate the magnitude of this disconnection, it has been reported that entry into torpor is associated with a 50–60% loss of synapses in the golden-mantled ground squirrel (*Callospermophilus lateralis*) (106). Thus, while some brain regions appear to remain functional during torpor, much of the brain is quiescent.

Importantly, synaptic connectivity and electrical activity in the brain are regained by IBA (106, 108), indicating that extensive synaptic restructuring is occurring during arousal. Studies in golden hamsters indicate that brain energy metabolism is maintained during arousal (67), suggesting that the brain is functioning during arousal as it would normally during homeothermy. However, synaptic plasticity and maintenance require extensive ATP production (7, 46), making arousal and IBA energetically costly periods (106). Additionally, because of the short duration of arousal (45), synaptic plasticity also has to occur very rapidly. Therefore, a major shift in energy demand occurs between torpor and IBA, a physiological transition that occurs many times throughout hibernation.

Overall, the exact mechanisms by which hibernators regulate their metabolism during hibernation are not fully understood. Mitochondria are a logical focal point to investigate metabolic regulation in hibernators, as they are the primary site for oxygen consumption and have considerable control over

energy-demanding processes (reviewed in Refs. 89 and 101). Therefore, mitochondria are integral to orchestrating the extreme changes in energy demand in the brain during hibernation. However, most of the mitochondrial metabolic studies have been done in ground squirrel liver, which shows significant suppression during torpor in thirteen-lined ground squirrels (reviewed in Ref. 101; Supplemental Table S1 and Refs. 3, 16, 19, 20, 23, 25, 26, 37, 40, 51, 53, 83, 99). Investigation of other tissues, like the brain, may provide insight into the overall metabolic mechanisms of ground squirrels and hibernators in general.

To withstand numerous shifts in energy demand during the hibernation season, we predict that unlike the liver, brain mitochondrial metabolism is not actively suppressed during hibernation compared with spring. There has only been one study investigating brain mitochondria in a hibernator, which found no difference in mitochondrial respiration rates in cerebral cortex between torpor and IBA (39). However, this study only investigated brain mitochondrial metabolism during hibernation, and no seasonal consideration was taken. By measuring mitochondrial metabolism throughout the year, our goal was to gain insight into the mechanisms and adaptations that the ground squirrel brain employs to maintain function during extreme physiological challenges and shifts in energy demand. Therefore, the aim of this study was to investigate the mitochondrial metabolism of the thirteen-lined ground squirrel brain both during and outside of the hibernation season.

MATERIALS AND METHODS

Animal capture and care. All procedures were approved by the University of Minnesota Institutional Animal Care and Use Committee (IACUC; protocol no. 1103A97712). Wild thirteen-lined ground squirrels, *Ictidomys tridecemlineatus*, were live-trapped on private property, with permission, near Paynesville, Minnesota, in 2013 and 2014. After capture, animals were housed in the American Association for Accreditation of Laboratory Animal Care-accredited animal care facility located in the University of Minnesota Duluth School of Medicine. Squirrels were housed individually in plastic top-load rat cages filled with aspen shavings. The squirrels were kept at room temperature in a 12:12-h light-dark cycle at 23°C and fed standard rodent chow (Purina, no. 5001) and water ad libitum. During the hibernation season (around November to March), the squirrels were moved into an artificial hibernation chamber and kept in constant darkness at 5–7°C with no food provided, but water was provided ad libitum.

Experimental collection points. An equal number of males and females were euthanized at each collection point: torpor (TOR), IBA, and post-hibernation (spring active, SP). A complete synopsis of the experimental collection points can be found in Schwartz et al. (96). Briefly, during hibernation, animals were monitored daily using the sawdust method (84). Animals used for the torpor sample point were around *day 4* into a torpor bout and had shown no signs of arousal. Torpid state was verified at sacrifice by rectal body temperature (6–8°C). All animals used for the IBA sample point aroused spontaneously, were observed as awake and active, and were torpid the previous day. All IBA collection point animals had a normothermic body temperature (35–37°C), as verified by rectal measurement at the time of death. Animals at the hibernation time point (torpor and IBA) were euthanized in December, January, and February, when average torpor bout length is longest (96). The spring-active time point provides an opportunity to examine the period of recovery after the completion of an entire hibernation season. Spring-active animals were sampled in April and May. April animals had undergone hibernation within the animal care facility, while May animals were collected from the field and presumably had undergone hibernation in the field.

All animals were deeply anesthetized with 5% isoflurane until unresponsive to a toe pinch and then euthanized by decapitation before tissue collection. Although torpid ground squirrels have a reduced respiratory rate, this experimental group was still exposed to the same anesthesia and toe pinch protocol, as per the University of Minnesota Duluth IACUC procedural approval. Isoflurane has been shown to have an effect on mitochondrial metabolism in mice treated with isoflurane for 3–6 h (111); however, we expect there to be no effect of our isoflurane treatment on brain mitochondria, as our squirrels were briefly exposed to isoflurane (<10 min). Whole brain was removed from the skull, and the meninges and blood vessels surrounding the brain were removed. The brain was immediately placed in ice-cold mitochondrial isolation buffer (MIB; 250 mM sucrose, 1 mM EGTA, 5 mM HEPES, pH ~7.2–7.4).

Mitochondrial isolation. Mitochondrial isolation was performed on whole brains via differential centrifugation, adapted and modified from established protocols (63, 100). The brain was minced on ice and homogenized with 10 passes in 30 ml of ice-cold mitochondrial isolation buffer (MIB; 250 mM sucrose, 1 mM EGTA, 5 mM HEPES, pH ~7.2–7.4) + 0.1% fatty acid-free BSA using a rotating loose-fitting Teflon pestle. The homogenate was filtered through three layers of sterile gauze and centrifuged at 1,000 *g* for 10 min at 4°C. Floating lipid was aspirated from the supernatant, which was transferred to a new prechilled centrifuge tube and centrifuged at 500 *g* for 10 min at 4°C. Any additional floating lipid was aspirated from the supernatant, which was transferred to a new prechilled centrifuge tube and centrifuged at 10,500 *g* for 10 min at 4°C. The supernatant was decanted, and any lipid adhering to the tubes was carefully removed using KimWipes. The pellet was resuspended, including the fluffy synaptosomal layer (100), in 30-ml ice-cold wash buffer (WB; 250 mM sucrose, 5 mM HEPES, pH ~7.2–7.4) + 0.1% fatty acid-free BSA and centrifuged at 12,000 *g* for 10 min at 4°C. The supernatant was decanted, and the mitochondrial pellet was resuspended, including the fluffy synaptosomal layer (100), in 30 ml of ice-cold WB and centrifuged at 12,000 *g* for 10 min at 4°C. The final mitochondrial pellet was suspended in a minimal volume of WB, transferred to a prechilled Eppendorf tube, and kept on ice until assayed. The protein concentrations of isolated mitochondria were determined via BCA protein assay (Thermo Scientific, no. 23255), according to the manufacturer's instructions, using BSA as a standard. Mitochondrial bioenergetics analyses were performed directly after mitochondrial isolation at 25°C, and each mitochondrial sample was analyzed for in vitro respiration rates, proton leak, and calcium uptake.

We used 25°C as the assay temperature because it is the temperature experienced midarousal, representing the point during arousal when brain mitochondria would presumably be at the most risk of damage and, thus, would need to work as effectively as possible. This temperature has also been used in previous mitochondrial studies (4, 15, 41, 66, 75), including the brain (72). Finally, measurements were made at 25°C because, in our experience, it is the optimal in vitro temperature that yields reliable respiration and bioenergetics measurements, and isolation of brain mitochondria from individual animals did not provide enough volume to assay more than one temperature for each experiment.

In vitro mitochondrial respiration. In vitro mitochondrial respiration rates were determined using a Clark-type oxygen electrode (Hansatech Instruments, King's Lynn, UK) calibrated to 25°C with air-saturated dH$_2$O and corrected for local atmospheric pressure. Unless otherwise stated, all compounds were dissolved in dH$_2$O.

Mitochondria were added in a final concentration of 0.5 mg protein/ml in 0.5 ml of respiration buffer (135 mM sucrose, 65 mM KCl, 5 mM KH$_2$PO$_4$, 2.5 mM MgCl$_2$, 5 mM HEPES, pH 7.2–7.4) at 25°C, while undergoing constant stirring (63, 100, 110). Maximal flux through various segments of the electron transport chain (ETC) were

determined under phosphorylating (*state 3*; Ref. 24) conditions with the addition of saturating ADP (200 nM), using specific substrates and inhibitors (110). Flux through complex I was measured using 5 mM glutamate and 5 mM malate (G/M). Succinate (SUC; 5 mM) and glycerol-3-phosphate (G3P; 5 mM) were added to stimulate flux through complexes II–IV. G3P activates mitochondrial respiration through the use of the mitochondrial G3P-dehydrogenase, which fuels the respiratory chain with electrons independent of complex I. The use of G3P as a fuel for mitochondrial respiration has been used in previous brain studies (28, 57). Each substrate (e.g., SUC and G3P) was assayed in separate experiments, with a total of three respiration experiments measured for each sample. Rotenone (2 mM, dissolved in ethanol; an ETC complex I inhibitor) was added to the mitochondrial suspension before SUC and G3P were introduced to prevent reverse electron flow. All substrate oxidation rates were allowed to reach both steady state 3 and steady state 4 (nonphosphorylating) respiration rates (24, 29). To assess the integrity of the mitochondrial inner membranes of our isolated mitochondrial fractions, we measured the respiratory control ratio (RCR). RCR is the ratio between state 3 and state 4, and it is an indicator of coupling efficiency between substrate oxidation and ATP synthesis (24, 110).

Membrane potential and proton leak. For the determination of proton leak kinetics, simultaneous measurements of oxygen consumption and membrane potential ($\Delta\Psi_m$) were required (81, 97). A Clark-type oxygen electrode determined oxygen consumption, while a tetraphenylphosphonium (TPP$^+$, a lipophilic cation)-sensitive electrode determined membrane potential. Initially, rotenone (2 mM; dissolved in ethanol) was added to inhibit complex I, and oligomycin (1 μg/ml, dissolved in ethanol) was added to inhibit ATP synthesis. As in previous studies (15, 17, 18), we did not use nigericin to eliminate ΔpH in our assay. Nigericin can alter mitochondrial respiration rate and reduce mitochondrial respiratory control ratios (5, 41, 58, 88). Mitochondria were added to the chamber at a final concentration of 0.5 mg/ml at 25°C. Mitochondria were incubated in respiration buffer, rotenone, and oligomycin for at least 1 min before TPP$^+$ additions (5, 41). Both a TPP$^+$ and a reference electrode (Hansatech Instruments) were inserted into the oxygen chamber to measure external [TPP$^+$]. The TPP$^+$ electrode was calibrated by making three additions of TPP$^+$ (1 mM); each addition increased external [TPP$^+$] by 1 μM. After calibration, state 4 respiration was induced by the addition of 10 mM succinate. The kinetics of proton leak were determined by inhibiting succinate oxidation stepwise by titrating 0.3 mM malonate until a complete inhibition was obtained, and then measuring this effect on $\Delta\Psi_m$.

$\Delta\Psi_m$ was calculated from external [TPP$^+$] using a modified Nernst equation (*Eq. 1*), adapted from (5, 58, 97):

$$\Delta\Psi_m = -59\log\left(\frac{[TPP^+]added - [TPP^+]external}{(0.001)(mg\ protein)([TPP^+]external)}\right) \quad (1)$$

[TPP$^+$]$_{external}$ is the concentration of TPP$^+$ outside of the mitochondria, and the value 0.001 represents the internal volume of the mitochondria (taken as 1.1 μl/mg protein) (43). As in previous studies (17, 18), we did not determine whether mitochondrial matrix volume changes with metabolic state. Overall, changes in mitochondrial matrix volume have little effect on membrane potential measurements when TPP$^+$ is used (92).

Calcium loading capacity. For estimation of calcium-loading capacity, rotenone (2 mM, dissolved in ethanol) and oligomycin (1 μg/ml, dissolved in ethanol) were initially added to inhibit complex I and ATP synthesis, respectively. Mitochondria were added to the chamber at a final concentration of 0.5 mg/ml at 25°C. Both a calcium (filled with 10 mM CaCl$_2$) and a reference electrode (Hansatech Instruments) were inserted into the oxygen chamber to measure external [CaCl$_2$]. The CaCl$_2^+$ electrode was calibrated by sequential additions of CaCl$_2$ solution (e.g., 20 μM, 20 μM, 40 μM, 80 μM, and 100 μM, total 260 μM). Once calibrated, succinate (10 mM) was

added to stimulate state 4 respiration. The estimation of calcium loading capacity was determined after calcium loading halted in the mitochondrial suspension (i.e., mitochondria released calcium back into the medium; Fig. 1). This Ca^{2+}-induced mitochondrial Ca^{2+} release indicates the opening of the mitochondrial permeability transition pore (MPTP), which was confirmed by adding cyclosporin A (1 μM), a specific inhibitor of the MPTP (13), to block the Ca^{2+} release (114). The calcium-loading capacity is expressed as micromoles of CaCl$_2$ per milligram of mitochondrial protein (114).

Mitochondrial DNA and nuclear DNA quantification via qPCR. To infer differences in mitochondrial abundance across seasons, mitochondrial DNA (mtDNA) to nuclear DNA (nuDNA) ratio measurements were analyzed between spring and hibernating samples (4, 49). Briefly, DNA was isolated from frozen cerebral cortex samples from $n = 6$ IBA and SP, using QIAmp DNA blood mini kit (no. 51104; Qiagen, Germantown, MD). Cerebral cortex was chosen for analysis, as it is the largest region of the brain, thus giving a better representation of mitochondrial abundance present throughout the whole brain. Samples were taken from animals with similar seasonal timing (torpor bout length and total amount of time in hibernation conditions) as the animals used for functional analyses. Before DNA precipitation, samples were sonicated to ensure unbiased DNA extraction of nuclear and mitochondrial DNA (71). Primer sequences from unique mitochondrial segments (ND1, NADH dehydrogenase subunit 1) and single copy nuclear genes (B2M, β-2-macroglobulin) were previously designed (4) and synthesized by Integrated DNA Technologies (Coralville, IA). Primer sequences were as follows: ND1 (F: 5′-TGTC-CCAATCTTAGTAGCCATAGCCTT-3′; R:5′-TGCGTCAGCAAA-
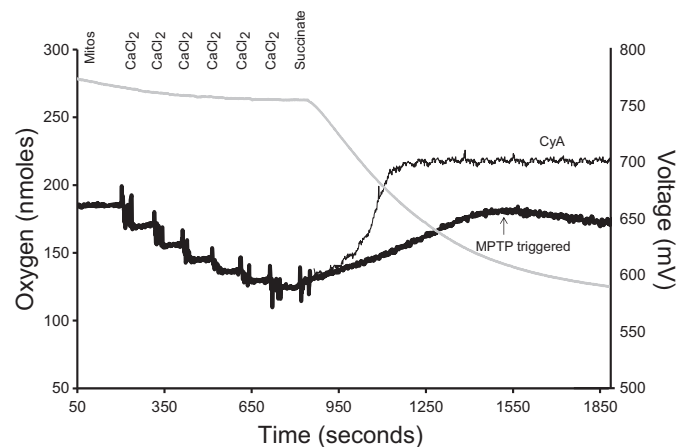

Fig. 1. A representative model for estimating calcium-loading capacity in isolated brain mitochondria. Mitochondrial calcium (black line traces) and oxygen consumption (gray line trace) were recorded simultaneously using a Clark-type oxygen electrode equipped with a CaCl$_2$-selective electrode. The calcium electrode measures extramitochondrial calcium as an electric potential between the assay media and the electrode filling solution, which contains 10 mM CaCl$_2$. In 1 ml of respiration buffer at 25°C, 0.5 mg mitochondria, rotenone (2 mM, dissolved in ethanol), and oligomycin (1 mg/ml, dissolved in ethanol) were added. Once a steady-state reading was established, sequential additions of CaCl$_2$ were made to calibrate the calcium electrode (20 μM, 20 μM, 40 μM, 80 μM, and 100 μM, total 260 μM). Additions of CaCl$_2$ are observed as a decrease in potential at the calcium electrode. When the mitochondria are energized (i.e., succinate addition), the calcium is sequestered in the mitochondria, which decreases the extramitochondrial CaCl$_2$ concentration, and is measured as an increase in electrical potential by the electrode. Calcium-loading capacity was estimated as the maximum amount of CaCl$_2$ sequestered by mitochondria before CaCl$_2$ loading halted (i.e., the mitochondrial permeability transition pore (MPTP) was triggered, indicated by thick, black line). Assay was repeated with the addition of 1 μM cyclosporin A (CyA, a specific inhibitor of MPTP) to confirm opening of MPTP through the blockage of CaCl$_2$ release back into the medium (indicated by thin, black line).
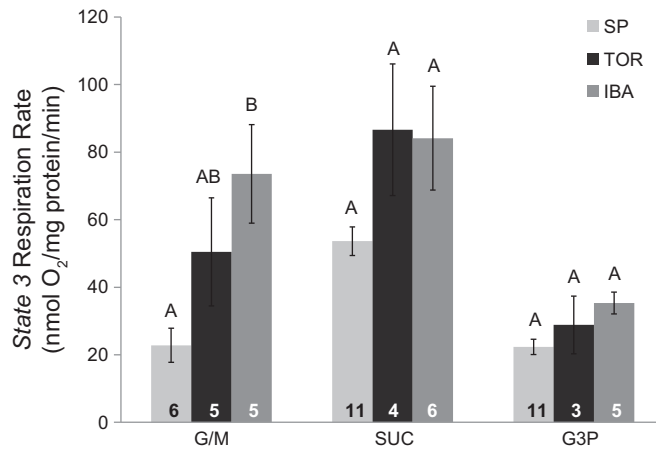
Fig. 2. Seasonal respiration rates in isolated brain mitochondria. State 3 respiration rates were measured at complexes I–III at 25°C. Time points at each complex that are not connected by the same letter are significantly different [Tukey's honestly signnificant difference (HSD) test, $P < 0.05$]. The number of samples for each group is indicated at the bottom in the corresponding bar. Data are expressed as means ± SE. G/M, glutamate/malate; G3P, glycerol-3-phosphate; SP, spring; SUC, succinate; TOR, torpor; IBA, interbout arousal; SE, standard error.

TGGTTGGAGT-3′) and B2M (F: 5′-ATACCCGGCACCCGGCT-GAG-3′; R:5′-AGAGAGGTCCGACTGCTCGACT-3′).

Target-specific standards for quantitative PCR (qPCR) were made by performing standard PCR reactions for each primer set using Amplitaq gold 360 hot start PCR master mix (Applied Biosystems, Foster City, CA). The PCR products were then purified using QIAquick PCR purification kit (no. 28104; Qiagen) and quantified by measuring the absorbance at 260 nm with a Nanodrop ND1000. Quantitative PCR was performed with the individual mitochondrial and nuclear primers on the RotorGene3000 (Qiagen) using qEvaGreen master mix (qARTA Bio, Carson, CA), in accordance with the procedure of Lutfalla and Uze (68). Each sample was run in duplicate along with a 5-point, 10-fold serial dilution of target specific standard. Crossing threshold values were derived following the procedures of Hampton et al. (44), and copy numbers of target-specific sample DNA were calculated using each target-specific standard curve. These values were used to calculate the ratio of ND1:B2M, or mitochondrial to nuclear DNA.

Data analysis. Statistical analyses were accomplished using JMP Pro 12 statistical software. Significant differences in seasonal respiration rates, calcium loading capacity, and mtDNA copy number between hibernating and spring samples were analyzed using one-way ANOVA and were considered significant at $P < 0.05$. Significant results from ANOVA tests were further analyzed using a Tukey's honestly significant difference (HSD) test to find means that were significantly different from each other ($P < 0.05$). P values presented in the results section are Tukey's HSD values. All data presented are means ± SE.

The relationships between respiration and membrane potential were graphed and compared between hibernating and spring groups, as described previously (5, 41). The maximal membrane potential and nonphosphorylating respiration rates were compared between hibernating and spring-active animals by a one-way ANOVA, and kinetic curves were compared by the overlap of standard error bars; the existence of no overlap was interpreted as a significant difference between curves (8, 14, 34, 41, 52).

RESULTS

Seasonal respiration rates. At complex I fueled with G/M, state 3 respiration rates were more than threefold higher in IBA

animals compared with SP animals, when measured at 25°C (one-way ANOVA, $P < 0.05$; Fig. 2). This same trend is also seen with complexes II–IV, where state 3 respiration rates with SUC and G3P have higher rates in TOR and IBA compared with SP, but these results were not significant [$P = 0.0542$ (SUC), $P = 0.0726$ (G3P)]. The rather small extent of G3P-dependent respiration indicates a low capacity of the G3P dehydrogenase in brain mitochondria, regardless of season. State 4 respiration rates (nmol O_2 mg^{-1}·protein·min^{-1}) using G/M for SP, TOR, and IBA were 9.14 ± 1.51, 21.38 ± 4.91, and 23.69 ± 3.65, respectively. Additionally, RCRs, used as an indicator of mitochondrial quality, were calculated using G/M as a substrate. The RCRs for SP, TOR, and IBA were 2.81 ± 0.35, 2.44 ± 0.38, and 3.13 ± 0.43, respectively. These values are comparable to RCRs of previous brain mitochondria studies (e.g., Ref. 6) and indicate well-coupled mitochondria.

Proton leak kinetics. Proton leak kinetics were determined at 25°C for SP, TOR, and IBA, and are summarized in Fig. 3. Proton leak kinetic curves for TOR and IBA were shifted down and to the right when compared with SP animals (Fig. 3). Maximal nonphosphorylating respiration rates (uppermost point in curves) did not differ significantly between spring and hibernating states, but the maximum membrane potential was significantly lower in SP (Fig. 3). Specifically, there was a significant increase in maximum $\Delta\Psi_m$ in TOR and IBA compared with SP (one-way ANOVA, $P < 0.001$). There were, however, no significant differences in maximal state 4 respiration rates, further supporting the state 3 and RCR data from respiration experiments. Additionally, there was a significant decrease in $\Delta\Psi_m$ in TOR and IBA compared with SP after the first addition of malonate (the second furthest points to the
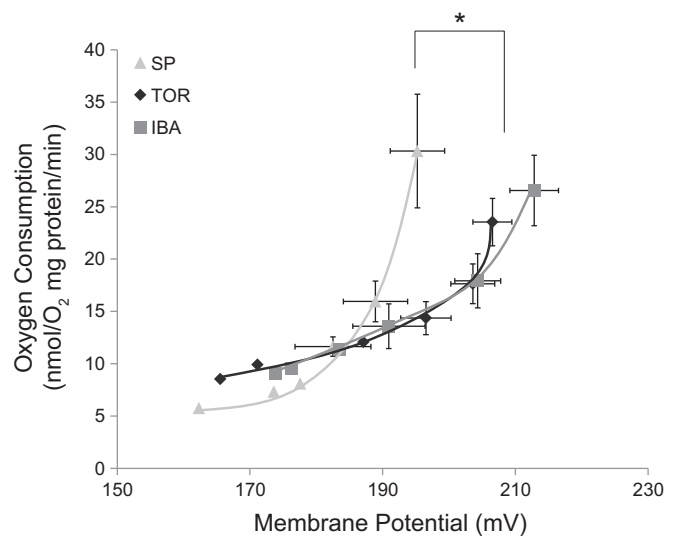

Fig. 3. Proton leak kinetics of brain mitochondria between spring and hibernation. Maximal state 4 conditions (respiration rate and $\Delta\Psi_m$) are shown as the upper right-most points. Proton leak kinetics were initiated by inducing state 4 respiration with the addition of 10 mM succinate. The kinetics of proton leak were determined by inhibiting succinate oxidation stepwise by titrating 0.3 mM malonate until a complete inhibition was obtained and then measuring this effect on $\Delta\Psi_m$ (see MATERIALS AND METHODS for details). Each data point represents the means of all individuals sampled for that time point (standard error bars were left out of last three data points for clarity). *Significant differences (Tukey's HSD test, $P < 0.05$) in maximal membrane potential (no malonate; the upper-right point of each curve). $\Delta\Psi_m$, membrane potential; SP, spring ($n = 6$); TOR, torpor ($n = 8$); IBA, interbout arousal ($n = 5$).

right in Fig. 3; one-way ANOVA, $P < 0.05$), further demonstrating the mitochondrial differences in the brain between hibernation and spring.

The highest $\Delta\Psi_m$ shared between SP, TOR, and IBA was ~195 mV, where proton leak is higher in SP than TOR/IBA (Fig. 3). In addition, SP had an overall higher proton leak compared with TOR and IBA and would be considered different by the criterion of nonoverlapping error bars and when comparing the fit of the two curves. This suggests that proton permeability of the mitochondrial membrane is higher in SP compared with hibernation.

Calcium loading capacity. A second parameter that we used to assess proton permeability and mitochondrial integrity was calcium-loading capacity (114). Because calcium plays important and dynamic roles in mitochondria (reviewed in Ref. 94), we investigated the seasonal differences in calcium uptake in brain mitochondria to gain a better understanding of how energy use and production differs between seasons. Isolated brain mitochondria of thirteen-lined ground squirrels were able to load significantly more calcium during SP compared with TOR and IBA (one-way ANOVA, $P = 0.0013$; Fig. 4). In the presence of cyclosporin A, mitochondria accumulated and retained all of the added $CaCl_2$ (see MATERIALS AND METHODS for details).

mtDNA copy number. To analyze brain mitochondrial abundance between spring and hibernation, we determined the ratio of copy number in a mitochondrial gene (*ND1*) vs. a nuclear gene (*B2M*) in frozen cerebral cortex samples. No significant differences were observed in DNA copies between SP and IBA (*t*-test, $P = 0.141$, data not shown). However, a trend shows that SP animals had a lower mtDNA copy number ratio compared with IBA (SP = 483.27 ± 39.35 copies; IBA = 639.07 ± 89.11 copies).

DISCUSSION

The brain is an important tissue that contributes roughly 5% to the overall energetic needs and metabolism of rodents (50),
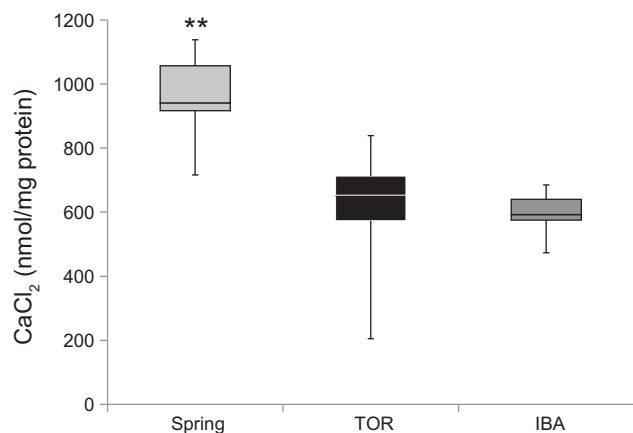

Fig. 4. Calcium-loading capacity of brain mitochondria. Assessment of calcium loading capacity was performed on isolated brain mitochondria from thirteen-lined ground squirrels. Briefly, $CaCl_2$ (260 μM) was titrated into the chamber upon the addition of succinate (10 mM) to stimulate approximately state 4 respiration (see MATERIALS AND METHODS for details). The estimation of calcium-loading capacity was determined after calcium loading halted in the mitochondrial suspension. SP, $n = 6$; TOR, $n = 7$; IBA, $n = 6$. **$P < 0.01$, Tukey's HSD.

including the thirteen-lined ground squirrel. Unlike other tissues, where metabolism is suppressed during torpor (reviewed in Ref. 101), maintenance of brain metabolism at some reduced level is critical because it is, in part, the central regulator of hibernation (31). This suggests an innate adaptation to maintain function in the brain during extreme physiological challenge (27). Here, we measured several bioenergetic properties of isolated brain mitochondria from the thirteen-lined ground squirrel to determine changes associated with seasonal variation in energy demand. The results of this study suggest that brain mitochondria during hibernation have increased capacity for oxidative phosphorylation compared with brain mitochondria during spring. This was evidenced by increases in flux fueled through complex I of the ETC, decreases in mitochondrial proton leak, and decreased calcium loading in hibernation.

Brain mitochondrial metabolism is not suppressed during hibernation at 25°C. Brain mitochondria isolated from thirteen-lined ground squirrels exhibit both high respiration rates and low proton leak during torpor and IBA when measured at 25°C, suggesting that brain mitochondrial substrate oxidation during hibernation is better coupled to ADP phosphorylation. No differences were found in mitochondrial function between torpor and IBA at 25°C, indicating that isolated brain mitochondria during the entire hibernation season are primed for rapid and improved ATP production. Using permeabilized tissues, Gallagher and Staples (39) also saw no change in mitochondrial function between torpor and IBA in the brain cortex. This is in contrast to other tissues, such as liver and skeletal muscle, that show a suppression of mitochondrial function during torpor when compared with IBA (reviewed in Ref. 101). A lack of mitochondrial suppression in the brain during torpor is intuitive since the brain is a major metabolic tissue that includes regions that signal and regulate important autonomic functions during hibernation, such as regulating metabolic rate (31, 98). In fact, high-energy phosphates in the brains of ground squirrels appear to be higher in torpor than IBA (47), suggesting that energy is being stored during torpor for future use during an arousal. Furthermore, the large ATP requirement for arousal is supported by this study as isolated brain mitochondria from hibernating animals show enhanced mitochondrial bioenergetics, such as lower proton leak.

It is important to note that this study only investigated isolated brain mitochondria at a single temperature (i.e., 25°C) and with only a subset of fuels. Because the ground squirrel brain preferentially uses ketones during hibernation (1), specific substrates, such as fatty acid derivatives, could play a role in the overall oxidative capacity of brain mitochondria across the year. For example, with more fatty acids being metabolized during hibernation, one would hypothesize that proton leak would be greater during hibernation, contrary to this study's findings. Future analyses should look at the effects of different substrates, namely ketones and fatty acids, on mitochondrial bioenergetics in the brain. Moreover, temperature has been shown to effect tissue-specific metabolism of isolated mitochondria in hibernators (reviewed in Ref. 101). For example, it was recently shown that brown adipose tissue mitochondrial respiration was enhanced at 25°C during hibernation compared with spring, but this capacity was decreased at lower temperatures [e.g., temperature coefficients (Q_{10}) effect was present] (4). Thus, measuring mitochondrial bioenergetics at one tem-

perature in this study limits the interpretation of our results. However, 25°C is the temperature experienced midarousal, representing the point during arousal when brain mitochondria would presumably be at the most risk of damage and, thus, would need to work as effectively as possible. Therefore, we believe seasonal differences seen at 25°C are important differences that speak to the nature of the hibernation biology in the brain.

Calcium regulation plays a significant role in mitochondrial metabolism. Mitochondrial calcium uptake is essential for mitochondrial function, including ATP production and various cellular signaling processes (30, 42, 87, 104; reviewed in Ref. 94). The direct uptake of calcium into the mitochondrial matrix via the mitochondrial calcium uniporter uses the proton gradient (73, 77, 82) and directly competes with mitochondrial ATP synthesis (78, 79). In fact, it has been shown that a high rate of Ca^{2+} uptake lowers the proton-motive force sufficiently to cause a transient reversal of the ATP synthase (9). Moreover, endogenous ATP is hydrolyzed to support accumulation of calcium into mitochondria (9). Because calcium uptake takes precedence over ADP phosphorylation in competition for the energy of respiration (91), the lack of calcium transport by mitochondria would potentially be an energy-producing process of physiological significance—a process necessary for hibernation.

During hibernation, brain mitochondria sequester significantly less calcium into the mitochondrial matrix compared with mitochondria during spring (Fig. 4), as indicated by the low-calcium loading capacity in hibernation. The reduced uptake and storage of calcium in the mitochondrial matrix during hibernation allows for a shift in utilization of the proton circuit, primarily for the essential ATP production needed for arousal from torpor to IBA. Indeed, it has recently been shown that neurons in hibernating Daurian ground squirrels (*Spermophilus dauricus*) are able to maintain lower levels of intracellular calcium concentrations compared with rats and, thus, are better at maintaining calcium homeostasis (113). Additionally, both Arctic ground squirrels and golden hamsters show downregulation of *N*-methyl-D-aspartate receptor function during hibernation (90, 112), blunting calcium responses, such as mitochondria-dependent apoptosis (60, 64). Finally, the disassembly of synapses occurring with each torpor bout in thirteen-lined ground squirrels is likely to complement the overall downregulation of ion channels to reduce the potential for calcium buildup at cold body temperatures and detrimental excitotoxicity (27, 48).

In addition to the supporting functional data presented here, transcriptomic and proteomic supporting data from thirteen-lined ground squirrel brain regarding calcium uptake are available. Schwartz et al. (96) saw significant increases in two genes related to calcium-binding (*SLC24A2* and *S100A6*) during hibernation in the cerebral cortex compared with spring. These two genes may play significant roles in binding and regulating calcium levels in the brain. Additionally, Hindle and Martin (48) showed sorcin protein, SRI (soluble resistance-related calcium binding protein), to be in low abundance at cold temperatures (i.e., torpor) in the forebrain of the thirteen-lined ground squirrel. SRI may be implicated in calcium homeostasis by regulating intracellular calcium handling during torpor (48). Taken together, future studies should characterize calcium dynamics and the role it plays in mitochondrial function of

hibernators. Specifically, dissecting both the torpor and IBA bouts at different temperatures may shed light onto how calcium regulates ATP demand, and how this compares to the active season.

Enhanced production of ATP aids in arousal. The various functional data accumulated in this experiment (e.g., high respiration rates, lower proton leak, and less calcium uptake) suggest that an improved production of ATP is occurring during hibernation, which is necessary for the energetically demanding arousals from torpor throughout hibernation. In support of these functional observations, Epperson et al. (36) identified upregulation of numerous mitochondrial proteins in the thirteen-lined ground squirrel brain stem during hibernation, also suggesting rapid ATP production upon arousal from torpor. Additionally, they also found a higher expression of mitochondrial membrane proteins (NDUFS1, NDUFS3, NDUFV2, UQCRC1, UQCRH, ATP5A1, ATP5B, and VDAC2) in early torpor (i.e., torpor occurring right after IBA) in the brain stem of thirteen-lined ground squirrels (36). Epperson et al. (36) found higher winter copy number of proteins in oxidative phosphorylation (such as complex I of the ETC), which allows brain mitochondria to rapidly and effectively produce ATP for arousal.

High respiration rates and less proton leak observed in brain mitochondria during hibernation promote the risk of producing reactive oxygen species (ROS). Mitochondria produce superoxide as a by-product of oxidative metabolism, and are a major source of intracellular ROS production (7, 11, 76). Because superoxide production is dependent on the proton-motive force (56, 59, 65), proton leak pathways may exist to mitigate the proton gradient and overall minimize oxidative damage (10, 29). Although this study did not directly measure the production of ROS from isolated mitochondria, one can predict that an enhanced function of brain mitochondria during hibernation produces ROS more readily than in the spring, and, thus, poses the risk for oxidative damage. However, it has been documented that hibernators have a suite of neuroprotective mechanisms in the brain during hibernation to minimize oxidative damage from ROS. For example, the synaptic dissociation that occurs during hibernation may serve a neuroprotective purpose (96). Recent Illumina HiSeq sequencing of the cerebral cortex transcriptome indicates that the brain upregulates transcripts important for plasticity and remodeling before hibernation onset (96). Additionally, mammalian hibernators exhibit a striking ability to tolerate oxidative stress during hibernation by eliminating free radicals generated during repeated cycles of torpor and arousal (102). It is known that hibernating ground squirrels and bats have antioxidant defense systems against oxidative stress (21, 27, 31–33, 80, 103, 109), and the amounts of antioxidant proteins vary among different stages of torpor-arousal cycles (21, 35, 61, 74, 107). In addition, melatonin receptor-mediated mechanisms have been shown to aid in mitochondrial performance of thirteen-lined ground squirrel brain during arousal from torpor (95). Specifically, inhibition of melatonin receptor signaling reduced state 3 respiration rates in brain mitochondria, thus, suggesting melatonin aids in the mitochondrial performance of rapid production of ATP during arousal (95). It is possible that melatonin production upon arousal from torpor functions to help brain mitochondria work more effectively during a period of extreme energy need (95).

Perspectives and Significance

This study provides additional insight into the overall metabolic system of the thirteen-lined ground squirrel. Moreover, it aids in the understanding of tissue-specific mitochondrial metabolism, which, until this study, very little investigation had been done on brain mitochondrial metabolism in hibernators. Similar to brown adipose tissue mitochondria (4), brain mitochondria exhibit an enhanced oxidative capacity during hibernation. Although the focus of this study was on seasonal changes of mitochondrial bioenergetics with one temperature and a few substrates, future studies should aim to understand the effects of temperature and fatty acid oxidation on the oxidative capacity of brain mitochondria across the year. Furthermore, future studies should focus on measuring mitochondrial bioenergetics in separate regions of the brain, which may aid in a better understanding of how different regions of a hibernator's brain adapt to the extreme physiological conditions associated with the hibernation phenotype. Finally, it was recently proposed that the ground squirrel brain contains neuronal uncoupling protein 1 (UCP1) to aid in local thermogenesis (60). Although we did not measure uncoupling rates of respiration with the use of fatty acid derivatives, our study does not support the presence of functional UCP1, as we see no evidence of the uncoupling associated with this protein. In fact, our data show that brain mitochondria are more tightly coupled in hibernation when compared with spring and that only basal proton leak was observed throughout hibernation in brain mitochondria. Although we hypothesize that there is no functionally active UCP1 in the brain, future studies should test this hypothesis with the additions of free fatty acids and GDP to detect UCP1-dependent proton leak.

DISCLOSURES

No conflicts of interest, financial or otherwise, are declared by the authors.

AUTHOR CONTRIBUTIONS

M.A.B., C.S., and M.T.A. conception and design of research; M.A.B. performed experiments and analyzed data; M.A.B., C.S., and M.T.A. interpreted results of experiments; M.A.B. prepared figures; M.A.B. drafted manuscript; M.A.B., C.S., and M.T.A. edited and revised manuscript.

REFERENCES

1. **Andrews MT, Russeth KP, Drewes LR, Henry PG.** Adaptive mechanisms regulate preferred utilization of ketones in the heart and brain of a hibernating mammal during arousal from torpor. *Am J Physiol Regul Integr Comp Physiol* 296: R383–R393, 2009. doi:10.1152/ajpregu.90795.2008.
2. **Andrews MT.** Advances in molecular biology of hibernation in mammals. *BioEssays* 29: 431–440, 2007. doi:10.1002/bies.20560.
3. **Armstrong C, Staples JF.** The role of succinate dehydrogenase and oxaloacetate in metabolic suppression during hibernation and arousal. *J Comp Physiol B* 180: 775–783, 2010. doi:10.1007/s00360-010-0444-3.
4. **Ballinger MA, Hess C, Napolitano MW, Bjork JA, Andrews MT.** Seasonal changes in brown adipose tissue mitochondria in a mammalian hibernator: from gene expression to function. *Am J Physiol Regul Integr Comp Physiol* 311: R325–R336, 2016. doi:10.1152/ajpregu.00463.2015.
5. **Barger JL, Brand MD, Barnes BM, Boyer BB.** Tissue-specific depression of mitochondrial proton leak and substrate oxidation in hibernating arctic ground squirrels. *Am J Physiol Regul Integr Comp Physiol* 284: R1306–R1313, 2003. doi:10.1152/ajpregu.00579.2002.
6. **Benani A, Barquissau V, Carneiro L, Salin B, Colombani AL, Leloup C, Casteilla L, Rigoulet M, Pénicaud L.** Method for functional study of mitochondria in rat hypothalamus. *J Neurosci Methods* 178: 301–307, 2009. doi:10.1016/j.jneumeth.2008.12.023.
7. **Boveris A, Chance B.** The mitochondrial generation of hydrogen peroxide. General properties and effect of hyperbaric oxygen. *Biochem J* 134: 707–716, 1973. doi:10.1042/bj1340707.
8. **Brand MD, Couture P, Else PL, Withers KW, Hulbert AJ.** Evolution of energy metabolism. Proton permeability of the inner membrane of liver mitochondria is greater in a mammal than in a reptile. *Biochem J* 275: 81–86, 1991. doi:10.1042/bj2750081.
9. **Brand MD, Lehninger AL.** Superstoichiometric Ca^{2+} uptake supported by hydrolysis of endogenous ATP in rat liver mitochondria. *J Biol Chem* 250: 7958–7960, 1975.
10. **Brand MD.** Uncoupling to survive? The role of mitochondrial inefficiency in ageing. *Exp Gerontol* 35: 811–820, 2000. doi:10.1016/S0531-5565(00)00135-2.
11. **Brand MD.** The sites and topology of mitochondrial superoxide production. *Exp Gerontol* 45: 466–472, 2010. doi:10.1016/j.exger.2010.01.003.
12. **Bratincsák A, McMullen D, Miyake S, Tóth ZE, Hallenbeck JM, Palkovits M.** Spatial and temporal activation of brain regions in hibernation: *c-fos* expression during the hibernation bout in thirteen-lined squirrel. *J Comp Neurol* 505: 443–458, 2007. doi:10.1002/cne.21507.
13. **Broekemeier KM, Dempsey ME, Pfeiffer DR.** Cyclosporin A is a potent inhibitor of the inner membrane permeability transition in liver mitochondria. *J Biol Chem* 264: 7826–7830, 1989.
14. **Brookes PS, Buckingham JA, Tenreiro AM, Hulbert AJ, Brand MD.** The proton permeability of the inner membrane of liver mitochondria from ectothermic and endothermic vertebrates and from obese rats: correlations with standard metabolic rate and phospholipid fatty acid composition. *Comp Biochem Physiol B Biochem Mol Biol* 119: 325–334, 1998. doi:10.1016/S0305-0491(97)00357-X.
15. **Brown JCL, Chung DJ, Belgrave KR, Staples JF.** Mitochondrial metabolic suppression and reactive oxygen species production in liver and skeletal muscle of hibernating thirteen-lined ground squirrels. *Am J Physiol Regul Integr Comp Physiol* 302: R15–R28, 2012. doi:10.1152/ajpregu.00230.2011.
16. **Brown JCL, Chung DJ, Cooper AN, Staples JF.** Regulation of succinate-fuelled mitochondrial respiration in liver and skeletal muscle of hibernating thirteen-lined ground squirrels. *J Exp Biol* 216: 1736–1743, 2013. doi:10.1242/jeb.078519.
17. **Brown JCL, Gerson AR, Staples JF.** Mitochondrial metabolism during daily torpor in the dwarf Siberian hamster: role of active regulated changes and passive thermal effects. *Am J Physiol Regul Integr Comp Physiol* 293: R1833–R1845, 2007. doi:10.1152/ajpregu.00310.2007.
18. **Brown JCL, Staples JF.** Mitochondrial metabolism during fasting-induced daily torpor in mice. *Biochim Biophys Acta* 1797: 476–486, 2010. doi:10.1016/j.bbabio.2010.01.009.
19. **Brown JCL, Staples JF.** Substrate-specific changes in mitochondrial respiration in skeletal and cardiac muscle of hibernating thirteen-lined ground squirrels. *J Comp Physiol B* 184: 401–414, 2014. doi:10.1007/s00360-013-0799-3.
20. **Brustovetsky NN, Mayevsky EI, Grishina EV, Gogvadze VG, Amerkhanov ZG.** Regulation of the rate of respiration and oxidative phosphorylation in liver mitochondria from hibernating ground squirrels, *Citellus undulatus*. *Comp Biochem Physiol B* 94: 537–541, 1989.
21. **Buzadžić B, Blagojević D, Korać B, Saičić ZS, Spasić MB, Petrović VM.** Seasonal variation in the antioxidant defense system of the brain of the ground squirrel (*Citellus citellus*) and response to low temperature compared with rat. *Comp Biochem Physiol C* 117: 141–149, 1997. doi:10.1016/S0742-8413(97)00061-3.
22. **Carey HV, Andrews MT, Martin SL.** Mammalian hibernation: cellular and molecular responses to depressed metabolism and low temperature. *Physiol Rev* 83: 1153–1181, 2003. doi:10.1152/physrev.00008.2003.

23. **Chaffee RRJ, Pengelley ET, Allen JR, Smith RE.** Biochemistry of brown fat and liver of hibernating golden mantled ground squirrels (*Citellus lateralis*). *Can J Physiol Pharmacol* 44: 217–223, 1966. doi:10.1139/y66-026.

24. **Chance B, Williams GR.** Respiratory enzymes in oxidative phosphorylation. III. The steady state. *J Biol Chem* 217: 409–427, 1955.

25. **Chung D, Lloyd GP, Thomas RH, Guglielmo CG, Staples JF.** Mitochondrial respiration and succinate dehydrogenase are suppressed early during entrance into a hibernation bout, but membrane remodeling is only transient. *J Comp Physiol B* 181: 699–711, 2011. doi:10.1007/s00360-010-0547-x.

26. **Cooper AN, Brown JCL, Staples JF.** Are long-chain acyl CoAs responsible for suppression of mitochondrial metabolism in hibernating 13-lined ground squirrels? *Comp Biochem Physiol B Biochem Mol Biol* 170: 50–57, 2014. doi:10.1016/j.cbpb.2014.02.002.

27. **Dave KR, Christian SL, Perez-Pinzon MA, Drew KL.** Neuroprotection: lessons from hibernators. *Comp Biochem Physiol B Biochem Mol Biol* 162: 1–9, 2012. doi:10.1016/j.cbpb.2012.01.008.

28. **Dineley KE, Richards LL, Votyakova TV, Reynolds IJ.** Zinc causes loss of membrane potential and elevates reactive oxygen species in rat brain mitochondria. *Mitochondrion* 5: 55–65, 2005. doi:10.1016/j.mito.2004.11.001.

29. **Divakaruni AS, Brand MD.** The regulation and physiology of mitochondrial proton leak. *Physiology (Bethesda)* 26: 192–205, 2011. doi:10.1152/physiol.00046.2010.

30. **Drago I, Pizzo P, Pozzan T.** After half a century mitochondrial calcium in- and efflux machineries reveal themselves. *EMBO J* 30: 4119–4125, 2011. doi:10.1038/emboj.2011.337.

31. **Drew KL, Buck CL, Barnes BM, Christian SL, Rasley BT, Harris MB.** Central nervous system regulation of mammalian hibernation: implications for metabolic suppression and ischemia tolerance. *J Neurochem* 102: 1713–1726, 2007. doi:10.1111/j.1471-4159.2007.04675.x.

32. **Drew KL, Osborne PG, Frerichs KU, Hu Y, Koren RE, Hallenbeck JM, Rice ME.** Ascorbate and glutathione regulation in hibernating ground squirrels. *Brain Res* 851: 1–8, 1999. doi:10.1016/S0006-8993(99)01969-1.

33. **Drew KL, Tøien Ø, Rivera PM, Smith MA, Perry G, Rice ME.** Role of the antioxidant ascorbate in hibernation and warming from hibernation. *Comp Biochem Physiol C* 133: 483–492, 2002. doi:10.1016/S1532-0456(02)00118-7.

34. **Duong CA, Sepulveda CA, Graham JB, Dickson KA.** Mitochondrial proton leak rates in the slow, oxidative myotomal muscle and liver of the endothermic shortfin mako shark (*Isurus oxyrinchus*) and the ectothermic blue shark (*Prionace glauca*) and leopard shark (*Triakis semifasciata*). *J Exp Biol* 209: 2678–2685, 2006. doi:10.1242/jeb.02317.

35. **Eddy SF, Storey KB.** Up-regulation of fatty acid-binding proteins during hibernation in the little brown bat, *Myotis lucifugus*. *Biochim Biophys Acta* 1676: 63–70, 2004. doi:10.1016/j.bbaexp.2003.10.008.

36. **Epperson LE, Rose JC, Russell RL, Nikrad MP, Carey HV, Martin SL.** Seasonal protein changes support rapid energy production in hibernator brainstem. *J Comp Physiol B* 180: 599–617, 2010. doi:10.1007/s00360-009-0422-9.

37. **Fedotcheva NJ, Sharyshev AA, Mironova GD, Kondrashova MN.** Inhibition of succinate oxidation and K^+ transport in mitochondria during hibernation. *Comp Biochem Physiol B* 82: 191–195, 1985.

38. **Frerichs KU, Kennedy C, Sokoloff L, Hallenbeck JM.** Local cerebral blood flow during hibernation, a model of natural tolerance to "cerebral ischemia". *J Cereb Blood Flow Metab* 14: 193–205, 1994. doi:10.1038/jcbfm.1994.26.

39. **Gallagher K, Staples JF.** Metabolism of brain cortex and cardiac muscle mitochondria in hibernating 13-lined ground squirrels *Ictidomys tridecemlineatus*. *Physiol Biochem Zool* 86: 1–8, 2013. doi:10.1086/668853.

40. **Gehnrich SC, Aprille JR.** Hepatic gluconeogenesis and mitochondrial function during hibernation. *Comp Biochem Physiol B* 91: 11–16, 1988.

41. **Gerson AR, Brown JCL, Thomas R, Bernards MA, Staples JF.** Effects of dietary polyunsaturated fatty acids on mitochondrial metabolism in mammalian hibernation. *J Exp Biol* 211: 2689–2699, 2008. doi:10.1242/jeb.013714.

42. **Glancy B, Balaban RS.** Role of mitochondrial Ca^{2+} in the regulation of cellular energetics. *Biochemistry* 51: 2959–2973, 2012. doi:10.1021/bi2018909.

43. **Halestrap AP.** The regulation of the matrix volume of mammalian mitochondria in vivo and in vitro and its role in the control of mitochondrial metabolism. *Biochim Biophys Acta* 973: 355–382, 1989. doi:10.1016/S0005-2728(89)80378-0.

44. **Hampton M, Melvin RG, Kendall AH, Kirkpatrick BR, Peterson N, Andrews MT.** Deep sequencing the transcriptome reveals seasonal adaptive mechanisms in a hibernating mammal. *PLoS One* 6: e27021, 2011. doi:10.1371/journal.pone.0027021.

45. **Hampton M, Nelson BT, Andrews MT.** Circulation and metabolic rates in a natural hibernator: an integrative physiological model. *Am J Physiol Regul Integr Comp Physiol* 299: R1478–R1488, 2010. doi:10.1152/ajpregu.00273.2010.

46. **Harris JJ, Jolivet R, Attwell D.** Synaptic energy use and supply. *Neuron* 75: 762–777, 2012. doi:10.1016/j.neuron.2012.08.019.

47. **Henry PG, Russeth KP, Tkac I, Drewes LR, Andrews MT, Gruetter R.** Brain energy metabolism and neurotransmission at near-freezing temperatures: in vivo ^{1}H MRS study of a hibernating mammal. *J Neurochem* 101: 1505–1515, 2007. doi:10.1111/j.1471-4159.2007.04514.x.

48. **Hindle AG, Martin SL.** Cytoskeletal regulation dominates temperature-sensitive proteomic changes of hibernation in forebrain of 13-lined ground squirrels. *PLoS One* 8: e71627, 2013. doi:10.1371/journal.pone.0071627.

49. **Hindle AG, Martin SL.** Intrinsic circannual regulation of brown adipose tissue form and function in tune with hibernation. *Am J Physiol Endocrinol Metab* 306: E284–E299, 2014. doi:10.1152/ajpendo.00431.2013.

50. **Hofman MA.** Energy metabolism, brain size and longevity in mammals. *Q Rev Biol* 58: 495–512, 1983. doi:10.1086/413544.

51. **Horwitz BA, Nelson L.** Effect of temperature on mitochondrial respiration in a hibernator (*Myotis austroriparius*) and a non-hibernator (*Rattus rattus*). *Comp Biochem Physiol* 24: 385–394, 1968. doi:10.1016/0010-406X(68)90990-0.

52. **Hulbert AJ, Else PL, Manolis SC, Brand MD.** Proton leak in hepatocytes and liver mitochondria from archosaurs (crocodiles) and allometric relationships for ectotherms. *J Comp Physiol B* 172: 387–397, 2002. doi:10.1007/s00360-002-0264-1.

53. **James RS, Staples JF, Brown JCL, Tessier SN, Storey KB.** The effects of hibernation on the contractile and biochemical properties of skeletal muscles in the thirteen-lined ground squirrel, *Ictidomys tridecemlineatus*. *J Exp Biol* 216: 2587–2594, 2013. doi:10.1242/jeb.080663.

54. **Kilduff TS, Miller JD, Radeke CM, Sharp FR, Heller HC.** 14C-2-deoxyglucose uptake in the ground squirrel brain during entrance to and arousal from hibernation. *J Neurosci* 10: 2463–2475, 1990.

55. **Kilduff TS, Sharp FR, Heller HC.** [14C]2-deoxyglucose uptake in ground squirrel brain during hibernation. *J Neurosci* 2: 143–157, 1982.

56. **Korshunov SS, Skulachev VP, Starkov AA.** High protonic potential actuates a mechanism of production of reactive oxygen species in mitochondria. *FEBS Lett* 416: 15–18, 1997. doi:10.1016/S0014-5793(97)01159-9.

57. **Kupsch A, Schmidt W, Gizatullina Z, Debska-Vielhaber G, Voges J, Striggow F, Panther P, Schwegler H, Heinze HJ, Vielhaber S, Gellerich FN.** 6-Hydroxydopamine impairs mitochondrial function in the rat model of Parkinson's disease: respirometric, histological, and behavioral analyses. *J Neural Transm (Vienna)* 121: 1245–1257, 2014. doi:10.1007/s00702-014-1185-3.

58. **Labajova A, Vojtiskova A, Krivakova P, Kofranek J, Drahota Z, Houstek J.** Evaluation of mitochondrial membrane potential using a computerized device with a tetraphenylphosphonium-selective electrode. *Anal Biochem* 353: 37–42, 2006. doi:10.1016/j.ab.2006.03.032.

59. **Lambert AJ, Brand MD.** Superoxide production by NADH:ubiquinone oxidoreductase (complex I) depends on the pH gradient across the mitochondrial inner membrane. *Biochem J* 382: 511–517, 2004. doi:10.1042/BJ20040485.

60. **Laursen WJ, Mastrotto M, Pesta D, Funk OH, Goodman JB, Merriman DK, Ingolia N, Shulman GI, Bagriantsev SN, Gracheva EO.** Neuronal UCP1 expression suggests a mechanism for local thermogenesis during hibernation. *Proc Natl Acad Sci USA* 112: 1607–1612, 2015. doi:10.1073/pnas.1421419112.

61. **Lee M, Choi I, Park K.** Activation of stress signaling molecules in bat brain during arousal from hibernation. *J Neurochem* 82: 867–873, 2002. doi:10.1046/j.1471-4159.2002.01022.x.

62. **Lerner E, Shug AL, Elson C, Shrago E.** Reversible inhibition of adenine nucleotide translocation by long chain fatty acyl coenzyme A esters in liver mitochondria of diabetic and hibernating animals. *J Biol Chem* 247: 1513–1519, 1972.

63. **Li Z, Graham BH.** Measurement of mitochondrial oxygen consumption using a Clark electrode. *Methods Mol Biol* 837: 63–72, 2012. doi:10.1007/978-1-61779-504-6_5.

64. **Lipton P.** Ischemic cell death in brain neurons. *Physiol Rev* 79: 1431–1568, 1999.

65. **Liu SS.** Generating, partitioning, targeting and functioning of superoxide in mitochondria. *Biosci Rep* 17: 259–272, 1997. doi:10.1023/A:1027328510931.

66. **Liu CC, Frehn JL, Laporta AD.** Liver and brown fat mitochondrial response to cold in hibernators and nonhibernators. *J Appl Physiol* 27: 83–89, 1969.

67. **Lust WD, Wheaton AB, Feussner G, Passonneau J.** Metabolism in the hamster brain during hibernation and arousal. *Brain Res* 489: 12–20, 1989. doi:10.1016/0006-8993(89)90003-6.

68. **Lutfalla G, Uze G.** Performing quantitative reverse-transcribed polymerase chain reaction experiments. *Methods Enzymol* 410: 386–400, 2006. doi:10.1016/S0076-6879(06)10019-1.

69. **Lyman CP, Willis JS, Malan A, Wang LCH.** *Hibernation and Torpor in Mammals and Birds.* New York: Academic, 1982.

70. **Magariños AM, McEwen BS, Saboureau M, Pevet P.** Rapid and reversible changes in intrahippocampal connectivity during the course of hibernation in European hamsters. *Proc Natl Acad Sci USA* 103: 18,775–18,780, 2006. doi:10.1073/pnas.0608785103.

71. **Malik AN, Shahni R, Rodriguez-de-Ledesma A, Laftah A, Cunningham P.** Mitochondrial DNA as a non-invasive biomarker: accurate quantification using real time quantitative PCR without co-amplification of pseudogenes and dilution bias. *Biochem Biophys Res Commun* 412: 1–7, 2011. doi:10.1016/j.bbrc.2011.06.067.

72. **Martin SL, Maniero GD, Carey C, Hand SC.** Reversible depression of oxygen consumption in isolated liver mitochondria during hibernation. *Physiol Biochem Zool* 72: 255–264, 1999. doi:10.1086/316667.

73. **Mitchell P, Moyle J.** Chemiosmotic hypothesis of oxidative phosphorylation. *Nature* 213: 137–139, 1967. doi:10.1038/213137a0.

74. **Morin P Jr, Storey KB.** Antioxidant defense in hibernation: cloning and expression of peroxiredoxins from hibernating ground squirrels, *Spermophilus tridecemlineatus*. *Arch Biochem Biophys* 461: 59–65, 2007. doi:10.1016/j.abb.2007.01.035.

75. **Muleme HM, Walpole AC, Staples JF.** Mitochondrial metabolism in hibernation: metabolic suppression, temperature effects, and substrate preferences. *Physiol Biochem Zool* 79: 474–483, 2006. doi:10.1086/501053.

76. **Murphy MP.** How mitochondria produce reactive oxygen species. *Biochem J* 417: 1–13, 2009. doi:10.1042/BJ20081386.

77. **Nicholls DG, Ferguson SJ.** *Bioenergetics* (4th ed.). New York: Elsevier, 2013.

78. **Nicholls DG.** Mitochondria and calcium signaling. *Cell Calcium* 38: 311–317, 2005. doi:10.1016/j.ceca.2005.06.011.

79. **Nicholls DG.** Mitochondrial calcium function and dysfunction in the central nervous system. *Biochim Biophys Acta* 1787: 1416–1424, 2009. doi:10.1016/j.bbabio.2009.03.010.

80. **Osborne PG, Hashimoto M.** Brain antioxidant levels in hamsters during hibernation, arousal and cenothermia. *Behav Brain Res* 168: 208–214, 2006. doi:10.1016/j.bbr.2005.11.007.

81. **Palmeira CM, Rolo AP.** Mitochondrial membrane potential ($\Delta\Psi$) fluctuations associated with the metabolic states of mitochondria. *Methods Mol Biol* 810: 89–101, 2012. doi:10.1007/978-1-61779-382-0_6.

82. **Pamenter ME.** Mitochondria: a multimodal hub of hypoxia tolerance. *Can J Zool* 92: 569–589, 2014. doi:10.1139/cjz-2013-0247.

83. **Pehowich DJ, Wang LCH.** Seasonal changes in mitochondrial succinate dehydrogenase activity in a hibernator, *Spermophilus richardsonii*. *J Comp Physiol B* 154: 495–501, 1984. doi:10.1007/BF02515154.

84. **Pengelley ET, Fisher K.** Rhythmical arousal from hibernation in the golden-mantled ground squirrel, *Citellus lateralis* tescorum. *Can J Zool* 39: 105–120, 1961. doi:10.1139/z61-013.

85. **Popov VI, Bocharova LS, Bragin AG.** Repeated changes of dendritic morphology in the hippocampus of ground squirrels in the course of hibernation. *Neuroscience* 48: 45–51, 1992. doi:10.1016/0306-4522(92)90336-Z.

86. **Popov VI, Bocharova LS.** Hibernation-induced structural changes in synaptic contacts between mossy fibres and hippocampal pyramidal neurons. *Neuroscience* 48: 53–62, 1992. doi:10.1016/0306-4522(92)90337-2.

87. **Rizzuto R, De Stefani D, Raffaello A, Mammucari C.** Mitochondria as sensors and regulators of calcium signalling. *Nat Rev Mol Cell Biol* 13: 566–578, 2012. doi:10.1038/nrm3412.

88. **Rolfe DF, Hulbert AJ, Brand MD.** Characteristics of mitochondrial proton leak and control of oxidative phosphorylation in the major oxygen-consuming tissues of the rat. *Biochim Biophys Acta* 1188: 405–416, 1994. doi:10.1016/0005-2728(94)90062-0.

89. **Rolfe DFS, Brown G.** Cellular energy utilization and molecular origin of standard metabolic rate in mammals. *Physiol Rev* 77: 731–758, 1997.

90. **Ross AP, Christian SL, Zhao HW, Drew KL.** Persistent tolerance to oxygen and nutrient deprivation and *N*-methyl-D-aspartate in cultured hippocampal slices from hibernating Arctic ground squirrel. *J Cereb Blood Flow Metab* 26: 1148–1156, 2006. doi:10.1038/sj.jcbfm.9600271.

91. **Rossi CS, Lehninger AL.** Stoichiometry of respiratory stimulation, accumulation of Ca^{++} and phosphate, and oxidative phosphorylation in rat liver mitochondria. *J Biol Chem* 239: 3971–3980, 1964.

92. **Rottenberg H.** Membrane potential and surface potential in mitochondria: uptake and binding of lipophilic cations. *J Membr Biol* 81: 127–138, 1984. doi:10.1007/BF01868977.

93. **Ruf T, Geiser F.** Daily torpor and hibernation in birds and mammals. *Biol Rev Camb Philos Soc* 90: 891–926, 2015. doi:10.1111/brv.12137.

94. **Santo-Domingo J, Demaurex N.** Calcium uptake mechanisms of mitochondria. *Biochim Biophys Acta* 1797: 907–912, 2010. doi:10.1016/j.bbabio.2010.01.005.

95. **Schwartz C, Ballinger MA, Andrews MT.** Melatonin receptor signaling contributes to neuroprotection upon arousal from torpor in thirteen-lined ground squirrels. *Am J Physiol Regul Integr Comp Physiol* 309: R1292–R1300, 2015.

96. **Schwartz C, Hampton M, Andrews MT.** Seasonal and regional differences in gene expression in the brain of a hibernating mammal. *PLoS One* 8: e58427, 2013. doi:10.1371/journal.pone.0058427.

97. **Servidio G, Sastre J.** Measurement of mitochondrial membrane potential and proton leak. *Methods Mol Biol* 594: 107–121, 2010. doi:10.1007/978-1-60761-411-1_7.

98. **Shibao C, Gamboa A, Diedrich A, Ertl AC, Chen KY, Byrne DW, Farley G, Paranjape SY, Davis SN, Biaggioni I.** Autonomic contribution to blood pressure and metabolism in obesity. *Hypertension* 49: 27–33, 2007. doi:10.1161/01.HYP.0000251679.87348.05.

99. **Shug AL, Ferguson S, Shrago E, Burlington RF.** Changes in respiratory control and cytochromes in liver mitochondria during hibernation. *Biochim Biophys Acta* 226: 309–312, 1971. doi:10.1016/0005-2728(71)90097-1.

100. **Silva AM, Oliveira PJ.** Evaluation of respiration with clark type electrode in isolated mitochondria and permeabilized animal cells. *Methods Mol Biol* 810: 7–24, 2012. doi:10.1007/978-1-61779-382-0_2.

101. **Staples JF.** Metabolic suppression in mammalian hibernation: the role of mitochondria. *J Exp Biol* 217: 2032–2036, 2014. doi:10.1242/jeb.092973.

102. **Storey KB.** Out cold: biochemical regulation of mammalian hibernation—a mini-review. *Gerontology* 56: 220–230, 2010. doi:10.1159/000228829.

103. **Tøien Ø, Drew KL, Chao ML, Rice ME.** Ascorbate dynamics and oxygen consumption during arousal from hibernation in Arctic ground squirrels. *Am J Physiol Regul Integr Comp Physiol* 281: R572–R583, 2001.

104. **Tomar D, Dong Z, Shanmughapriya S, Koch DA, Thomas T, Hoffman NE, Timbalia SA, Goldman SJ, Breves SL, Corbally DP, Nemani N, Fairweather JP, Cutri AR, Zhang X, Song J, Jaña F, Huang J, Barrero C, Rabinowitz JE, Luongo TS, Schumacher SM, Rockman ME, Dietrich A, Merali S, Caplan J, Stathopulos P, Ahima RS, Cheung JY, Houser SR, Koch WJ, Patel V, Gohil VM, Elrod JW, Rajan S, Madesh M.** MCUR1 is a scaffold factor for the MCU complex function and promotes mitochondrial bioenergetics. *Cell Reports* 15: 1673–1685, 2016. doi:10.1016/j.celrep.2016.04.050.

105. **von der Ohe CG, Darian-Smith C, Garner CC, Heller HC.** Ubiquitous and temperature-dependent neural plasticity in hibernators. *J Neurosci* 26: 10,590–10,598, 2006. doi:10.1523/JNEUROSCI.2874-06.2006.

106. **von der Ohe CG, Garner CC, Darian-Smith C, Heller HC.** Synaptic protein dynamics in hibernation. *J Neurosci* 27: 84–92, 2007. doi:10.1523/JNEUROSCI.4385-06.2007.

107. **Vucetic M, Stancic A, Otasevic V, Jankovic A, Korac A, Markelic M, Velickovic K, Golic I, Buzadzic B, Storey KB, Korac B.** The impact of cold acclimation and hibernation on antioxidant defenses in the ground squirrel (*Spermophilus citellus*): an update. *Free Radic Biol Med* 65: 916–924, 2013. doi:10.1016/j.freeradbiomed.2013.08.188.

108. **Walker JM, Glotzbach SF, Berger RJ, Heller HC.** Sleep and hibernation in ground squirrels (*Citellus* spp): electrophysiological observations. *Am J Physiol Regul Integr Comp Physiol* 233: R213–R221, 1977.

109. **Yin Q, Ge H, Liao CC, Liu D, Zhang S, Pan YH.** Antioxidant defenses in the brains of bats during hibernation. *PLoS One* 11: e0152135, 2016. doi:10.1371/journal.pone.0152135.

110. **Zhang J, Nuebel E, Wisidagama DR, Setoguchi K, Hong JS, Van Horn CM, Imam SS, Vergnes L, Malone CS, Koehler CM, Teitell MA.** Measuring energy metabolism in cultured cells, including human pluripotent stem cells and differentiated cells. *Nat Protoc* 7: 1068–1085, 2012. doi:10.1038/nprot.2012.048.

111. **Zhang Y, Xu Z, Wang H, Dong Y, Shi HN, Culley DJ, Crosby G, Marcantonio ER, Tanzi RE, Xie Z.** Anesthetics isoflurane and desflurane differently affect mitochondrial function, learning, and memory. *Ann Neurol* 71: 687–698, 2012. doi:10.1002/ana.23536.

112. **Zhao HW, Ross AP, Christian SL, Buchholz JN, Drew KL.** Decreased NR1 phosphorylation and decreased NMDAR function in hibernating Arctic ground squirrels. *J Neurosci Res* 84: 291–298, 2006. doi:10.1002/jnr.20893.

113. **Zhao JJ, Gao S, Jing JZ, Zhu MY, Zhou C, Chai Z.** Increased Na^+/Ca^{2+} exchanger activity promotes resistance to excitotoxicity in cortical neurons of the ground squirrel (a hibernator). *PLoS One* 9: e113594, 2014. doi:10.1371/journal.pone.0113594.

114. **Zhou S, Starkov A, Froberg MK, Leino RL, Wallace KB.** Cumulative and irreversible cardiac mitochondrial dysfunction induced by doxorubicin. *Cancer Res* 61: 771–777, 2001.